

K&C Science Report – Phase 2

Using ALOS/PALSAR, RADARSAT-2 and ENVISAT/ASAR Imagery to Define Threatened Species Habitats in the Pantanal

Maycira Costa*

*University of Victoria
(maycira@uvic.ca)

Teresa Evans*

(tevens@uvic.ca)

Walfrido Tomas**

Brazilian Government Agency – EMBRAPA (tomasw@cpap.embrapa.br)

Thiago Silva***

(thiago@uvic.ca)

Brazilian Institute of Space Science

Kevin Telmer*

(ktelmrr@uvic.ca)



K&C Science Report – Phase 2

Using ALOS/PALSAR, RADARSAT-2 and ENVISAT/ASAR Imagery to Define Threatened Species Habitats in the Pantanal

Maycira Costa*

*University of Victoria

(maycira@uvic.ca)

Teresa Evans*

(tevans@uvic.ca)

Walfrido Tomas**

Brazilian Government Agency – EMBRAPA (tomasw@cpap.embrapa.br)

Thiago Silva***

(thiago@uvic.ca)

Brazilian Institute of Space Science

Kevin Telmer*

(ktelmrr@uvic.ca)

Abstract — The Brazilian Pantanal is a large continuous tropical wetland with large biodiversity and many threatened habitats. The interplay between the distribution of vegetation, the hydrology, the climate and the geomorphology nourishes and sustains the large diversity of flora and fauna in this wetland, but it is poorly understood at the scale of the entire Pantanal. This study uses multi-temporal L-band ALOS/PALSAR and C-band RADARSAT-2 and ENVISAT/ASAR data to map ecosystems and create a lake distribution map of the Nhecolandia region in the Brazilian Pantanal. A Level 1 object-based image analysis (OBIA) classification defining fresh and brackish lakes was achieved with accuracy results of 98%. A Level 2 classification separating two types of fresh lakes and brackish lakes achieved with accuracy results of 81%. The preliminary analysis of distribution of lakes in relationship to the marsh deer distribution showed that during the dry season, the marsh deer are in close proximity to permanent waterways such as the Rio Negro (Southern border of Nhecolândia) and the Rio Taquari (North-western border of Nhecolândia). During the flood season the deer begin to migrate away from the more deeply flooded low-lying areas and into the shallower, seasonally flooded areas, following the flooded/dry interface. However, the deer do not migrate into the central part of Nhecolândia, suggesting that the aquatic vegetation

found in the *baías* alone is not enough to sustain the deer's diet, regardless of season.

Index Terms—ALOS PALSAR, K&C Initiative, Wetlands Theme, Pantanal, wildlife habitats.

I. INTRODUCTION

The Pantanal is the world's largest tropical wetland covering approximately 160,000km² (larger than England) and is located between Brazil, Paraguay and Bolivia. The Paraguay River, its tributaries, and the rainfall patterns of the region, support an annual flood regime that varies both temporally and spatially, and helps define the geomorphology in the region [1]. The geomorphological and hydrological diversity of this region promote a unique landscape characterized by different compositions of savanna vegetation, abundant species of aquatic vegetation, different types of floodplain forests [2],[3], and a large number of hydrochemically varied lakes, and waterways [4], [5],[6]. This complexity of ecosystems results in an abundance of biodiversity [1]. However, the Pantanal and its rich biodiversity are vulnerable to anthropogenic disturbances including the construction of hydroelectric dams, channelization of major waterways, and deforestation and burning of grasslands for agriculture and cattle ranching [1],

[7], [8]. Environmental degradation in the Pantanal is becoming an issue and requirements for more comprehensive studies of the different habitats and their relationships with the hydrological cycle of the Pantanal are needed. Although there have been several previous habitat studies at a local scale in the Pantanal [9],[10], only a few have covered the entire Pantanal at a regional scale [11], as the size and relative inaccessibility of the region hinders traditional methods of data collection. The primary goal of this research is to define on a regional scale the distribution of the variety of lakes in the Nhecolândia sub-region and their relationship with the marsh deer (*Blastocerus dichotomus*) population. To accomplish this we used fine resolution ALOS/PALSAR, RADARSAT-2 and ENVISAT/ASAR imagery acquired at different months over the Pantanal region.

II. DESCRIPTION OF YOUR PROJECT

A. Relevance to the K&C drivers

The primary goal of this research is to define on a regional scale the distribution of the variety of lakes in the Nhecolândia sub-region and their relationship with the marsh deer population. The following are the specific objectives:

1. Mosaic imagery data acquired from different satellites at different spatial resolutions;
2. Define the seasonal backscattering variability of the geochemically different lakes
3. Apply an object based image analysis (OBIA) classification to map the lakes;
4. Apply spatial analysis techniques to define areas preferentially used by the marsh deer, importance of lakes for marsh deer, and to define corridors and connectivity for conservation areas; (on-going)
5. Apply the methodology to the entire Pantanal using the 50m resolution mosaics. (on-going)

Objectives 1, 2, and 3 have been accomplished, and we are presently merging marsh deer data with the map of lakes distribution (4); the next step will be the analysis of the 50 m mosaic data (5).

The stated objectives are focused on providing quantifiable, accurate data for the purposes of improving management strategies of wild life habitat, and threats to which these habitats are exposed to, in the Pantanal. The outcomes are directly related to at least two “thematic drivers” of the K&C Initiative to support Conventions and Conservation.

B. Work approach

Study area

The Nhecolândia region is located in the south Pantanal, at approximately 19°00'S/56°12'W. It is bordered by the Negro River to the south and the Taquari River to the north (Fig 1). Nhecolândia experiences a monomodal flooding cycle, with

high waters occurring Feb-April, and low waters Aug-Nov [11]. The region has a highly heterogeneous and dynamic landscape, with forest, savanna, wild grasslands, introduced pastures, seasonal waterways, herbaceous vegetation, aquatic macrophytes and numerous lakes locally called *baías*, *salobras* and *salinas*, all occurring in close proximity to each other (Fig. 1).

The Nhecolândia region contains tens of thousands of lakes, generally divided into three categories: two classes of fresh water lakes (locally known as *baías* and *salobras*), and brackish lakes (locally known as *salinas*) [4]. *Baías* and *salobras* vary in size seasonally, typically expanding and connecting through water channels in the high water season, and shrinking considerably in the dry season. *Baías* are populated by a variety of floating/emergent aquatic vegetation and typically exhibit a fairly low pH and TDS concentration. *Salobras* can also be populated by floating and emergent aquatic vegetation, but are distinguished from *baías* by stands of *Typhaceae*. *Salobras* generally have a higher pH and TDS concentration than the majority of *baías*. *Salinas* tend to be permanent, rounded depressions ~500-1000m in diameter, 0.5-3.0m lower in elevation than *baías* and *salobras*, and are cut off from the flood by sandy barriers (*cordilheiras*) rising 2-3 meters higher than the *salinas* [12]. *Salinas* are devoid of any emergent aquatic vegetation and show the highest values of both pH and TDS compared to the other two lake types.

The emergent aquatic vegetation of these lakes essentially falls into two categories: blade-leaved, and broad-leaved plants. The first group is comprised of erectophile plants with blade-like leaves that are densely rooted and grass like. They range in height from 30-300cm tall and are populated by *Cyperaceae* (including *Eleocharis sp.*, *Scirpus sp.* and *Cyperus sp.*), and *Typhaceae* (including *Typha domingensis*) [4]; occurrence of *Typha sp.* is restricted to *salobras*. The second group of broad-leaved plants are floating emergent species that can occur in dense or relatively sparse stands, range in height from 2-30cm tall, and are dominated by *Pontederiaceae* (*Pontedera sp.*, *Eicchornia sp.*), *Araceae* (*Pistia stratiotes*), *Salviniaceae* (*Salvinia auriculata*), and *Nymphaeaceae* (*Nymphaea sp.*) [3],[4],[6]. This class of broad-leaved vegetation can be either rooted floating plants or free-floating plants, and represent the primary vegetal biomass, and an important primary producer of the Pantanal [6].

This variety of vegetation is a key component to the marsh deer's diet, which is chiefly composed of aquatic plants and/or by plants characteristic of wet and flooded habitats, including a significant portion of those species found in freshwater lakes (*Cyperaceae*, *Pontederiaceae*, *Nymphaeaceae*)[9]. The deer frequent habitats with inundation depths lower than 70cm, and typically range from low-lying areas along permanent waterways in the dry season to slightly higher elevations in flood season, following the seasonally dynamic ecotones between aquatic and terrestrial habitats [10].

Out of the hydrological regions in the Pantanal, the Nhecolândia region was chosen for this study because: it has a

high diversity of habitats; it has the highest number of lakes represented from all three categories; both L and C-band imagery were obtainable for both the high and low water season; primary ground reference data has already been collected for this region coinciding with dry season image acquisition for both L and C-band.

Field data

Field data were acquired for 75 lakes in July of 2008. Preliminary analysis of 2007 ALOS PALSAR imagery, Landsat ETM, and field data acquired in 2001, provided the approximate location of regions to be visited for this campaign. In addition, 55 lakes from the 2001 campaign were also used as ground reference data for this classification. Lake vegetation characteristics (species and distribution) were determined from direct observation, then recorded and photographed for each location. A handheld multiparameter Y.S.I (model 556) was used to collect conductivity, pH, and temperature for the lakes, and water samples from these lakes were taken to determine TDS concentrations. Alkalinity of the lakes was measured in the field using a HACH digital titrator. The collected data was organized into a database with geographic coordinates for each site. The lakes were divided into three categories (floating and emergent vegetation only; presence of *Typha sp.*; no vegetation), and alternating lakes in each category were assigned to training data or test data. From a total of 130 lakes, 7 were not usable for this study as they fell outside of the Nhecolândia border; from the remaining, 60 were used for training samples, and 61 were held back as testing samples for subsequent accuracy assessment.

Further, spatial distribution of different ground cover (forest, grasslands, agriculture, aquatic vegetation, open water, savanna) and vegetation characteristics (approximate height and dominant species) for a radius of approximately 100 m were determined, photographed, and recorded in visual observation diagrams for 209 additional sampling sites. Photographs included differing vegetation species/cover, and north, east, south and west views at each sampling site. This data was used as ground truth to define classification rules for separating lakes from other landscapes. Geographic location for each lake and sampling site was recorded using a Global Positioning System (GPS) receiver, with accuracy of 15-30 meters.

Marsh deer location data was provided by Walfrido Tomas of The Brazilian Agricultural Research Corporation (EMBRAPA). The data was collected from aerial survey with a Cessna airplane, using the double count technique as a strategy to correct detectability less than 1. This is a standard technique that used in the Pantanal and other wetlands in Brazil [10]. The data was collected from parallel transects with 30 km in length, spaced 3 km from each other. This data taken from a collection spanning 1991-2008, and month/year was included for each set of coordinates.

Satellite data

L-band images from ALOS/PALSAR were acquired for January/February 2008 (12.5m, HH polarization) coinciding with high water, and for August/September 2008 (12.5m, HH and HV polarization) coinciding with low water and the field campaign. ALOS/PALSAR images were acquired as part of the ALOS Kyoto and Carbon Initiative – Pantanal. C-band images from RADARSAT-2 were acquired for August 2008 (25m, HH and HV polarization) coinciding with low water and field campaign. Additional C-band data for high water was acquired in February/March 2010 from ENVISAT/ASAR (12.5m, HH and HV polarization). General characteristics of the data are provided in Table 1.

Images from all three sensors were acquired at a pre-processed level, and thus already radiometrically calibrated for incidence angle and radiometric distortions [14],[15],[16].

Water Geochemistry Analysis

Water samples from each of the lakes were collected in a depth of approximately 20cm and were immediately filtered on site through Millipore 0.22µm MCE (mixed cellulose esters) membranes, then preserved and properly stored until analysis in the laboratory. Alkalinity of the samples was measured in the field by titration using a HACH digital titrator, and pH and conductivity were determined on site using a handheld multiparameter Y.S.I (model 556).

Major dissolved cations and anions were analyzed in the laboratory using a Dionex DX-600 ion chromatograph. Total Dissolved Solids (TDS mg/L) were comprised of the total cation and anion content, as well as the alkalinity measured in the field.

Imagery processing

Step 1: Radiometric calibration

ALOS/PALSAR level 1.5 image files were processed using calibration tools made available by the Alaskan SAR facility, using provided geometric and radiometric data. RADARSAT-2 level 1-SGF images were processed and orthorectified using PCI Orthoengine, a SAR specific satellite orbiting model. ENVISAT/ASAR level 1P images were processed using calibration tools provided in the Next ESA SAR toolbox, a calibration software package provided by the European Space Agency (ESA). All data was converted to standardized backscatter coefficient intensity images.

Step 2: Geometry and mosaicking

Primary data geocoding was executed using provider software packages (mentioned above). Images were georeferenced and projected to UTM coordinates (zone 21, row K) using the WGS84 reference ellipsoid. Each set of images (L-band Feb 2008 HH; L-band Aug 2008 HH; L-band Aug 2008 HV, etc.) were mosaicked to form cohesive coverage of the study area. Cross-sensor geometric inconsistencies were corrected using the RADARSAT-2 mosaic as a master and

using a second order polynomial approach. All images were projected to UTM coordinates (Zone 21S), using the WSG84 reference ellipsoid. The Nhecolândia region vector based on Hamilton et al [11] (from EMBRAPA) was then utilized to delineate the study area from the mosaics.

Step 3: Speckle Filtering

Images were filtered to reduce the effect of speckle by utilizing a Kuan filter with a 3 x 3 kernel [17]. The resultant imagery showed preservation of the mean values, while decreasing the standard deviation of homogenous targets, and visually preserving the feature edges.

Step 4: OBIA Classification and Backscattering Analysis:

The classification was performed using an OBIA approach, executed using the eCognition software package (V.8.0). Generally, OBIA processing involves two main steps: multi-resolution segmentation and classification of resultant objects based on user defined rules. The multi-resolution segmentation algorithm in eCognition is controlled by three user-defined parameters: *scale*, *shape* and *compactness*. The *scale* parameter determines the maximum allowable heterogeneity of the image objects, and varies the size of the resulting image objects: larger scale values produce larger objects. The *shape* parameter determines the degree of influence of radiometry versus object shape in the delineation of image objects. Inputs values range between 0-1; smaller values result in objects optimized for radiometric homogeneity, higher values optimize for shape homogeneity [18]. *Compactness* also varies between 0 and 1, and determines the degree of smoothing for object borders. Different sets of parameters were tested, and optimal values selected separately for the classification of lakes in the Nhecolândia region. The general approach was as follows:

A primary multiresolution segmentation was performed using an optimal set of parameters for this stage: scale = 50 (resulting in objects that represented landscape features such as small lakes as individual entities, while not providing too fine a detail as to overload the software); shape = 0.005 (heavily emphasizing radiometry over shape); compactness = 0.5 (equal emphasis on smoothness and compactness); and, more heavily weighting the dry season imagery to better separate the lakes from seasonal flooding areas. To separate lakes from the rest of the terrain, sample training objects for “lakes” (fresh water floating and emergent vegetation; *Typha sp.*; open water) and “not lakes” (forest; grass/agriculture; savanna; seasonally flooded waterways) were chosen based on field data, and then a supervised classification using a combination of hierarchical rules and nearest neighbour parameters was performed. This primary classification was aided by the analysis of backscattering variability of observed land cover in the field for defined land covers of the Nhecolândia [19]. Everything classified as “not lake” was removed from subsequent analysis.

Mean values and standard deviations were exported for training site image objects from the three lake types and converted to normalized backscattering coefficients (σ^0)

expressed in dB. The conversion process for ALOS/PALSAR (from DN values) is as follows:

$$\sigma^0 = 10 * \log_{10} (DN^2) + CF \quad (\text{Equation 1})$$

where CF is the calibration coefficient for PALSAR standard products, and equals -83 dB [20].

For RADARSAT-2 images (from intensity values), conversion was performed as follows:

$$C = (DN^2 + B) / A \quad (\text{Equation 2})$$

where C is the calibrated value; B is the offset; and A is the range-dependant gain, both supplied in the LUT file [21]. The calibrated values were then expressed in dB via the following calculation:

$$\sigma^0 = 10 * \log(C) \quad (\text{Equation 3})$$

For ENVISAT/ASAR images (from intensity values), σ^0 was derived from the absolute calibration constant (K) from measurements over precision transponders via the following calculation (this step was performed by the NEST software package)[16]:

$$\sigma_{i,j}^0 = \frac{DN_{i,j}^2}{K} \sin(\alpha_{i,j}) \quad (\text{Equation 4})$$

where K = absolute calibration constant

$DN_{i,j}$ = pixel intensity value at image line and column “i,j”

$\sigma_{i,j}$ = sigma nought at image line and column “i,j”

$\alpha_{i,j}$ = incidence angle at image line and column “i,j”

The calibrated values were then expressed in dB via Equation 3.

Two levels of classification were produced as follows:

Level 1 Lakes Classification:

Based on the backscattering analysis and the image objects created in the primary classification, the lakes class was divided into fresh water lakes (lakes with only floating and emergent vegetation, as well as lakes with the presence of *Typha sp.*) and brackish lakes (lakes with no vegetation).

Level 2 Classification:

The creation of a Level 2 lakes classification was achieved by creating a mask for everything but the lakes to exclude it from further analysis. A new segmentation was performed, using the same parameters as the primary segmentation, however this time, the scale parameter was lowered to 10 to allow for much finer image objects, and a more detailed classification. A hierarchical classification scheme was developed using a myriad of rules based on mean backscattering, standard deviation, and area of image objects, as well as proximity parameters. The same training lakes used in the Level 1 classification were utilized for Level 2, but the more refined image objects allowed for greater distinction between floating and emergent vegetation, and stands of *Typha*

sp., that may have been combined in a single image object in Level 1. Some water channels that connect fresh water lakes in the flood season were erroneously classified as lake in the Level 1 classification; however, the finer scale segmentation at Level 2 allowed for the identification and removal of these areas, thereby further refining the lakes as individual entities.

At this time, the marsh deer point location data was split into dry and flood season and overlaid with the classification maps for spatial analysis.

Step 5: Validation of the classification results

Validation of the Level 2 lakes classification results was performed using the half of the field lake data held back for testing purposes. Lakes classified as having emergent/floating aquatic vegetation only were classed *baías*; lakes exhibiting either *Typha sp.* alone, or a combination of *Typha sp.* and emergent/floating aquatic vegetation were classified as *salobras*, and lakes showing open water/no vegetation were classified as *salinas*.

III. RESULTS AND SUMMARY

Water Geochemistry Analysis

Ranges for both TDS and pH for the three classes of lake/vegetation were determined by plotting TDS vs. pH on a simple scatterplot, and separating the lakes based on vegetation characteristics (Fig. 2); thus, a relationship between water geochemistry and vegetation was established.

Level 1 classes (vegetation/fresh water and no vegetation/brackish water) were clearly separable in terms of pH. The Level 1 freshwater class encompassed all lakes with vegetation, both floating/emergent, and with the presence of *Typha sp.*, and the brackish class contained all lakes with no vegetation. From the sampled lakes, all lakes with vegetation had a pH value of approximately ≤ 9 , and those with no vegetation ≥ 9 . Grouping via TDS was not as well defined; in general, fresh water lakes contained total TDS ≤ 500 mg/L, and brackish ≥ 500 mg/L, but with a few outliers.

The Level 2 classification attempted to distinguish between lakes with floating/emergent vegetation only, and those lakes with the presence of *Typha sp.* While no clear-cut separation was found to distinguish these two lakes types by either TDS or pH, there appeared to be an optimal range within which the presence of *Typha sp.* could be found: pH $\sim 6.8-8$, and TDS 100-500mg/L (excluding one outlier with much lower pH).

Backscattering separability of the lakes

Backscattering analysis was performed using the training objects from the three lake categories to determine which band/polarization/season was best able to separate the three lake types (Fig. 3).

Floating/emergent vegetation exhibited moderate to high backscattering variability, regardless of band or season. Mean backscattering values for this vegetation class were approximately -15 dB at L-band, HH for both flood and dry season, and -25 dB for L-band HV, and the variability was

somewhat higher in the dry season. For C-band, variability was lower, but mean backscattering was higher in the wet season at both polarizations (-7dB for HH and -15dB for HV in flood compared to -10dB HH and -18dB HV for dry).

Typha sp. exhibited the highest overall mean backscattering values for all imagery, ranging from approximately -5 dB for L-band HH dry season, and C-band HH both seasons, to -10dB L-band HH flood season, to -15dB for HV polarizations, both bands, both seasons. *Typha sp.* showed the highest variability in the L-band HH flood image, but variability was fairly low across all of the imagery.

Open water exhibited the lowest backscattering values and the lowest variability overall for all imagery. Mean backscattering values were approximately -22dB at L-band HH, flood and dry seasons, -30dB and at HV polarization, dry season. Open water was slightly more variable at C-band than at L-band, and backscattering was slightly higher (-17 to -20dB for HH and -20 to -25dB HV, both seasons).

Overall, open water was most separable from the vegetation classes based on mean backscattering at C-band, particularly in the flood season HH image, and based on variability in the L-band HH flood season image. Although no clear separation was apparent between floating/emergent water vegetation and *Typha sp.*, L-band dry season imagery (both HH and HV) showed the most difference between the two classes in terms of both mean backscattering and variability.

Lakes Classification

The Level 1 OBIA classification map shows the broad distribution of fresh and brackish lakes in the Nhecolândia region of the Pantanal (Fig. 4). An overall accuracy of 98% was achieved at this level. The only misclassification at this level was a single *baía* classified as a *salina*, likely a result of minimum of aquatic vegetation at the edges of a large, deep lake being mixed in the same pixels as the surrounding terrain. However, there were also three very small lakes in the testing data that were erroneously classified as “not lake” in the primary stage. This was likely due to a combination of factors: the scale parameter chosen for this stage may not have been fine enough to capture lakes of this size; lakes may have been desiccated at the time of image acquisition (3-6 weeks later than field campaign) thus causing confusion between the lakes and the surrounding terrain.

The Level 2 classification map shows the finer separation of aquatic vegetation into floating/emergent and *Typha sp.* classes, thus allowing the further distinction between *baías*, and *salobras*, and retaining the *salinas* from Level 1 (Fig. 5). For this level, an overall accuracy of 81% was achieved. The largest confusion, and thus the lowest producer’s accuracy (56%) and low user’s accuracy (75%), was for the *Salobra* class, where a little less than half of *salobras* observed in the field were misclassified as *baías*. This confusion is a result of several factors: the stand of *Typha sp.* observed in a lake in the field may have been too small to be captured as a single

object in the segmentation; the stand of *Typha sp.* may have been sparse and mixed with other aquatic vegetation, thereby reducing the backscattering signal considerably; *Typha sp.* stands observed in the 2001 field campaign may no longer be present, or may have been reduced in size and/or density.

The Level 2 classification shows the greatest concentration of *salinas* to be in the south-central/south-east portion of Nhecolândia, and dispersing towards the northwest. The spatial distribution of these lakes appears to follow diagonal lines (SW→NE) running perpendicular to the general direction of dispersion. *Salobras* follow the same general pattern as *salinas*; however they are also distributed in western Nhecolândia, where *salinas* are sparse. *Baixas* are evenly distributed across the entire region; however, they gain in size towards the east.

Marsh Deer Spatial Distribution

Preliminary visual inspection and interpretation of the spatial distribution of the marsh deer show a seasonal trend in movement consistent with that reported in Tomas et al [10]. During the dry season, the majority of location points are located in close proximity to permanent waterways such as the Rio Negro (Southern border of Nhecolândia) and the Rio Taquari (North-western border of Nhecolândia). During the flood season the deer begin to migrate away from the more deeply flooded low-lying areas and into the shallower,

seasonally flooded areas, following the flooded/dry interface. However, the deer do not migrate into the central part of Nhecolândia, suggesting that the aquatic vegetation found in the *baías* alone is not enough to sustain the deer's diet, regardless of season. However, a more in depth analysis of the marsh deer distribution in regard to the different habitats in the region is required. This is our next step by incorporating the 50m mosaics and classification of other important habitats in the Pantanal.

This project will provide vital habitat information for determining refuge zones for terrestrial species; connectivity of aquatic habitats during the dry season and implications for aquatic dependent species; examination of species distribution as a result of a flood-pulse regime; and risks of environmental changes to the animal population. Thus, by delineating habitat suitable to threatened species, such as the marsh deer, this study will help to define conservation strategies for the region.

ACKNOWLEDGEMENTS

The authors would like to acknowledge the K&C group for the valuable technical information. We also would like to thank you Ricardo Rossin for the geochemistry analysis. "This work has been undertaken within the framework of the JAXA Kyoto & Carbon Initiative. ALOS PALSA data have been provided by JAXA EORC."

REFERENCES

- [1] W. J. Junk, C. N. da Cunha, K. M. Wantzen, P. Peterman, C. Strussman, M. I. Marques, and J. Adis, "Biodiversity and its conservation in the Pantanal of Mato Grosso, Brazil," *Aquatic Sci.*, vol. 68, no. 3, pp. 278-309, Oct. 2006.
- [2] M.M. Abdon, V.J. Pott and J.S.V. Silva, "Evaluation of aquatic vegetation on ponds of Nhecolândia subregion in the Pantanal through Landsat and SPOT data," *Pesquisa Agropecuaria Brasileira*, vol. 33 pp. 1675-1681, 1998.
- [3] J. Pott, A. Pott, *Plantas aquáticas do pantanal*, Brazil, EMBRAPA, pp. 152, 2000.
- [4] M. P. F. Costa and K. H. Telmer, "Utilizing SAR imagery and aquatic vegetation to map the fresh and brackish lakes in the Brazilian Pantanal," *Remote Sens. Environ.*, vol. 105, no. 3, pp. 204-213, Dec. 2006.
- [5] M. Mariot, Y. Dudal, S. Furian, A. Sakamoto, V. Vallès, M. Fort, and L. Barbiero, "Dissolved organic matter fluorescence as a water-flow tracer in the tropical wetland of Pantanal of Nhecolândia, Brazil," *Sci. Total Environ.*, vol. 388, no. 1-3, pp. 184-193, Sept. 2007.
- [6] F. D. Por, *The Pantanal of Mato Grosso (Brazil): World's Largest Wetlands*. Monographiae Biologicae. Vol 73. Dumont H J & Werger M J A (eds). Kluwer:Dordrecht, 1995.
- [7] M. B. Harris, W. Tomas, G. Mourao, "Safeguarding the Pantanal wetlands: Threats and conservation initiatives," *Conserv. Biol.*, vol. 19, no. 3, pp. 714-720, Jun. 2005.
- [8] C. J. R. Alho, "Biodiversity of the Pantanal: response to seasonal flooding regime and to environmental degradation," *Brazilian J. Biol.*, vol. 68, No. 4, pp. 957-966, Nov. 2008.
- [9] W. M. Tomas and S. M. Salis, "Diet of the marsh deer (*Blastocerus dichotomus*) in the Pantanal wetland, Brazil," *Stud. Neotrop. Fauna & Environm.* vol. 35, pp. 165-172, 2000.
- [10] W. M. Tomas, S. M. Salis, M. P. da Silva, G. de Miranda Mourao, "Marsh deer (*Blastocerus dichotomus*) distribution as a function of floods in the Pantanal wetland, Brazil," *Stud. Neotrop. Fauna & Environm.* vol. 36, no. 1, pp. 9-13, 2001.
- [11] S. K. Hamilton, S. J. Sippel and J. M. Melack, "Inundation patterns in the Pantanal wetland of South America determined from passive microwave remote sensing," *Archiv Fur Hydrobiologie*, vol. 137, no. 1, pp. 23, Jul. 1996.
- [12] L. Barbiero, J. P. de Queiroz Neto, G. Ciornei, A. Y. Sakamoto, B. Capellari, E. Fernandes, V. Valles, "Geochemistry of water and groundwater in the Nhecolândia, Pantanal of Mato Grosso, Brazil: variability and associated processes," *Wetlands*, vol. 22, no. 3, pp. 528-540, September, 2002.
- [13] W. M. Tomas, M. D. Beccaceci, L. Pinder, "Cervo-do-Pantanal (*Blastocerus dichotomus*)," In: Duarte JMB, ed. *Biologia e conservacao de cervideos sul-americanos*, Jaboticabal, FUNEP, pp. 24-40.
- [14] A. Luscombe, "Image quality and calibration of Radarsat-2," *Proc. IGARSS*, Cape Town, South Africa, vol. 2, pp. 757-760, Jul. 2009.
- [15] M. Shimada, O. Isoguchi, T. Tadono, and K. Isono, "PALSAR Radiometric and Geometric Calibration," *IEEE Trans. Geosci. Remote Sens.*, vol. 47, no. 12, pp. 3915-3932, Dec. 2009.
- [16] B. Rosich and P. Meadows, "Absolute calibration of ASAR level 1 products generated with PF-ASAR," Technical note, ENVI-CLVL-EOPG-TN-03-0010, issue 1/5, October, 2004.
- [17] C. Oliver and S. Quegan, *Understanding synthetic aperture radar images*. Raleigh, NC. SciTech Publishing, Inc, 2004.
- [18] T. Esch, M. Thiel, M. Bock, A. Roth, and S. Dech, "Improvement of image segmentation accuracy based on multiscale optimization procedure," *IEEE, Geosci. Remote Sens. Lett.*, Vol. 5, no. 3, pp. 463-467, Jul. 2008.
- [19] T. L. Evans, M. Costa, K. Telmer, T. S. F. Silva, "Using ALOS/PALSAR and RADARSAT-2 to map land cover and seasonal inundation in the Brazilian Pantanal," *IEEE Journal of Selected Topics in Applied Earth Observations and Remote Sensing*, vol. 3, no. 4, pp. 560-575, December, 2010.
- [20] A. Rosenqvist, M. Shimada, N. Ito, and M. Watanabe, "ALOS PALSAR: A pathfinder mission for global-scale monitoring of the environment," *IEEE Trans. Geosci. Remote Sens.*, vol. 45, no. 11, pp. 3307-3317, Oct. 2007.
- [21] MacDonald, Dettwiler and Associates Ltd. RADARSAT-2 Product Format Definition. RN-RP-51-2713. Issue 1/7: Mar. 14, 2008.

Table 1 – SAR image dataset characteristics

SAR Imagery Dataset Characteristics									
Sensor	Processing Level	Band	Polarization	Spatial Resolution (m)	Swath Width (km)	Incidence Angle (°)	dates (dd/mm/yyyy)	scene ID (frame-path)	Season
ALOS PALSAR fine beam mode	1.5	L-band (23.6cm)	HH	12.5	40	34.3	27/01/2008	74-6790	Flood
								74-6800	
								74-6810	
							01/02/2008	77-6790	
								77-6800	
								75-6790	
							13/02/2008	75-6800	
								75-6810	
		01/03/2008	76-6790						
			76-6800						
			76-6810						
		HH/HV	29/07/2008				74-6790	Dry	
							74-6800		
							74-6810		
15/08/2008	75-6790								
	75-6800								
	75-6810								
01/09/2008	76-6790								
	76-6800								
18/09/2008	76-6810								
	77-6790								
ENVISAT ASAR ASA_APP_1P	1P	C-band (5.5cm)	HH/HV	12.5	30	36	11/02/2010	439-3987	Flood
								439-4005	
							27/02/2010	167-3987	
								167-4005	
							15/03/2010	396-3987	
								396-4005	
RADARSAT-2 S4 beam mode	1-SGF	C-band (5.5cm)	HH/HV	25	25	36.5	04/08/2008	91715	Dry
								91728	
								91741	
							11/08/2008	91304	
								91317	
								91330	
RADARSAT-2 S5 beam mode						39.2	22/11/2008	90901	
								90913	
								90927	

Table 2 – Accuracy Assessment

Level 1					
	Fresh Water	Brackish Water	Total	Producer's Accuracy	User's Accuracy
Fresh Water	46	1	47	98%	100%
Brackish Water	0	11	11	100%	92%
Total	46	12	58		

Level 2						
	Baia	Salobra	Salina	Total	Producer's Accuracy	User's Accuracy
Baia	27	3	1	31	87%	79%
Salobra	7	9	0	16	56%	75%
Salina	0	0	11	11	100%	92%
Total	34	12	12	58		

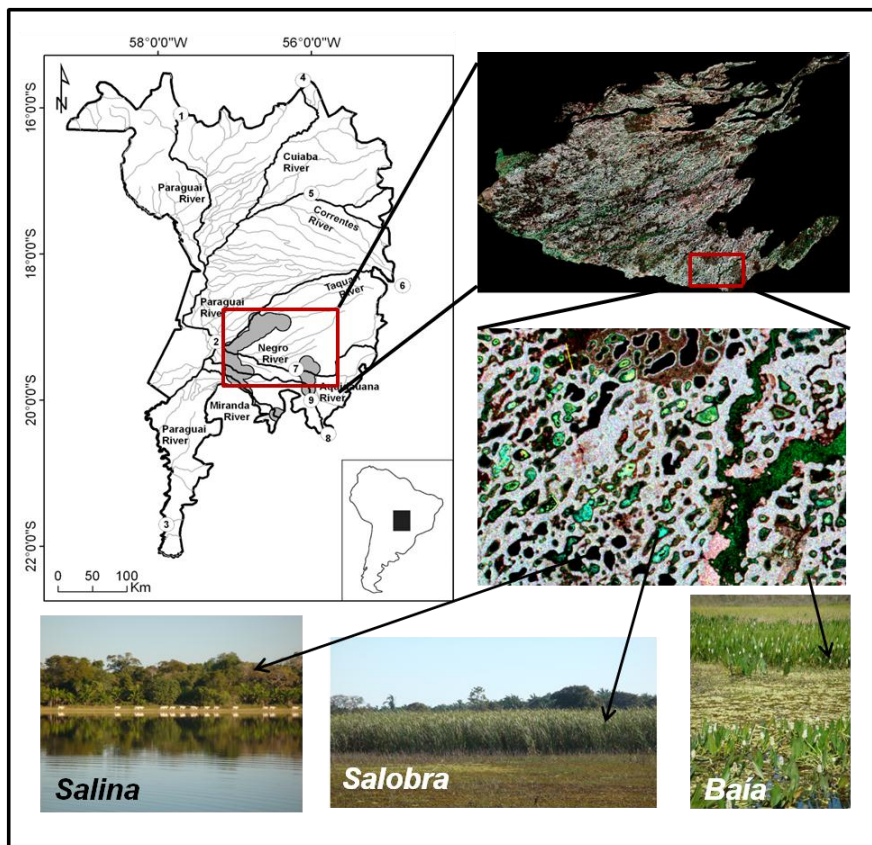


Figure 1 – Study Area

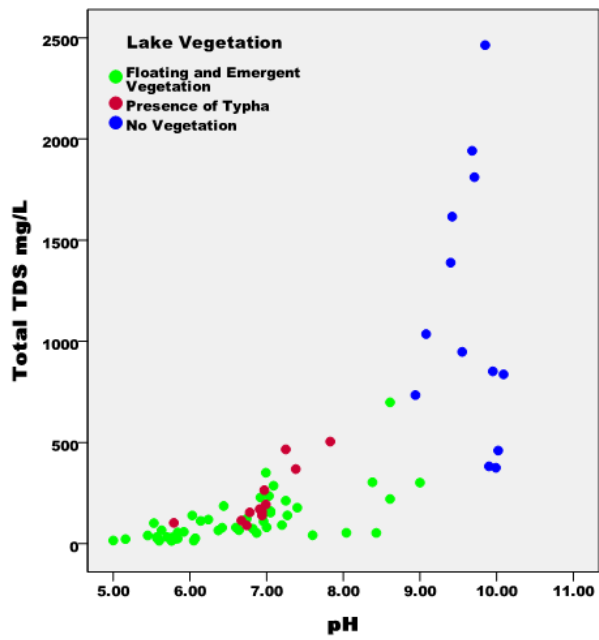


Figure 2 – Lake Geochemistry

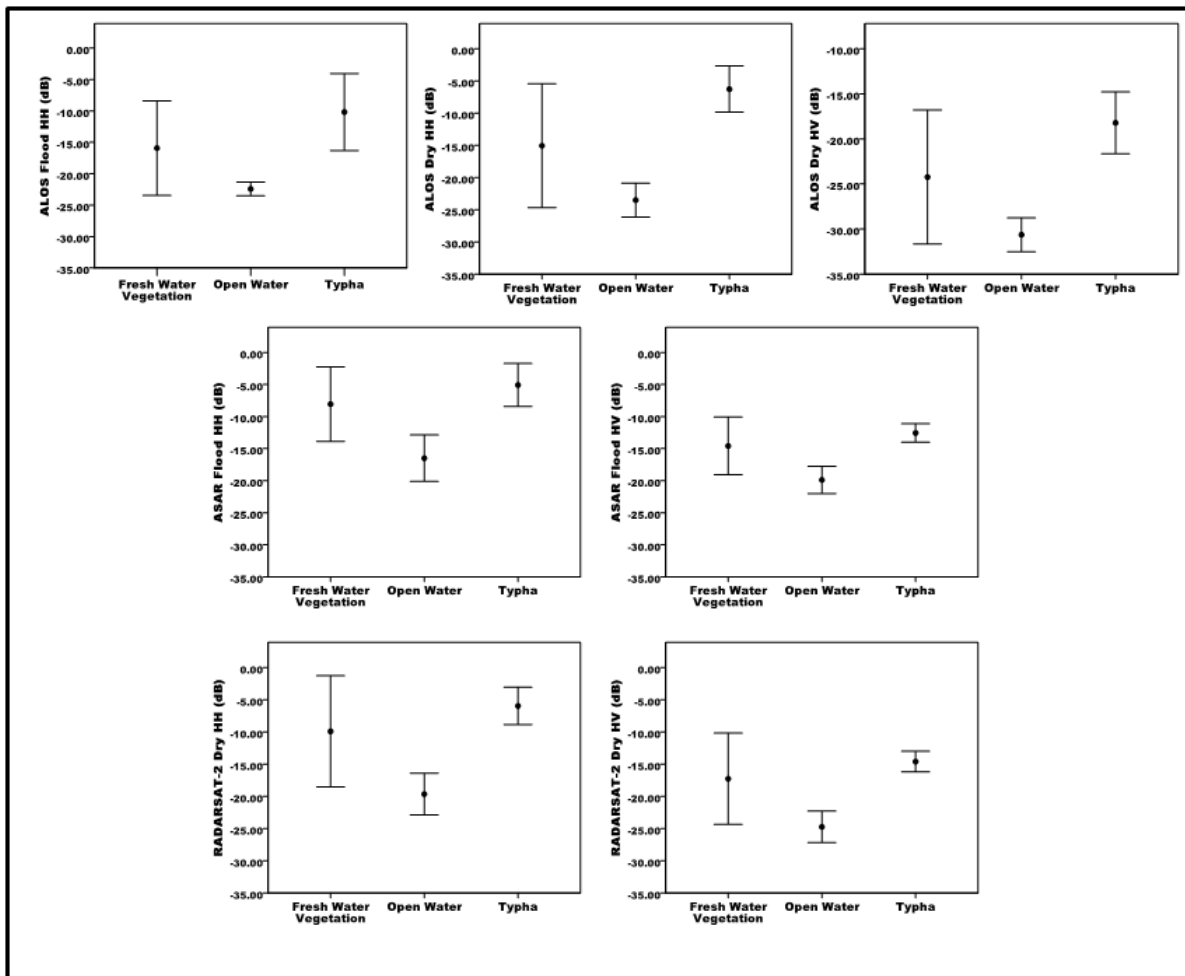


Figure 3 – Lake Vegetation Backscattering

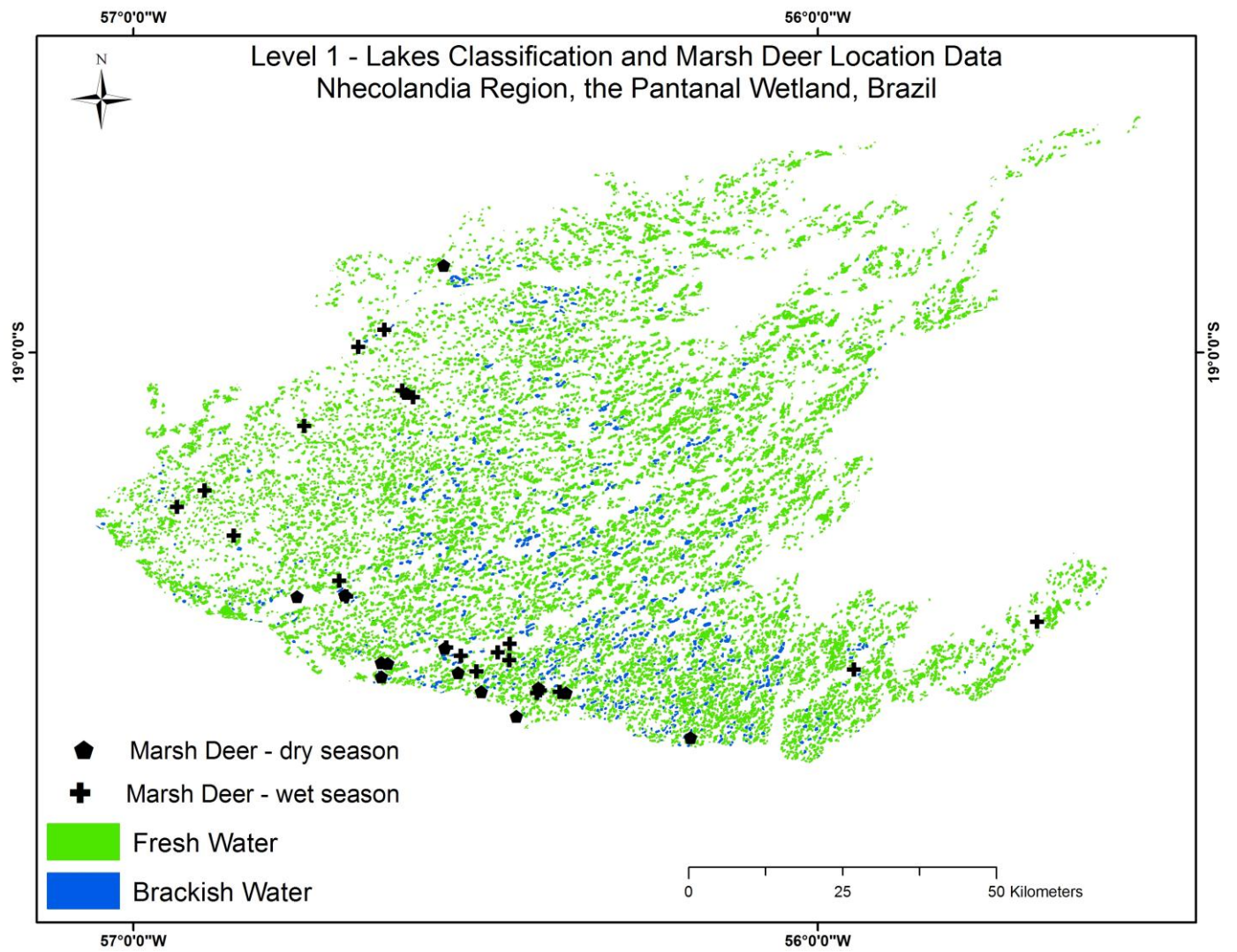


Figure 4 – Level 1 Lake Classification

APPENDIX 1

Field Sample Lake Geochemistry

Lake Vegetation Code: 1 - Fresh Water Vegetation;
2 – *Typha sp.*; 3 - No Vegetation/Open Water

Sample Name	pH	Total TDS (mg/L)	Lake Vegetation
1	6.94	158.10	2
2	6.67	114.59	2
3	6.96	164.27	1
4	9.42	1616.28	3
5	7.2	92.08	1
6	5.57	32.71	1
7	5.45	40.75	1
8	6.24	119.43	1
9	9.08	1035.94	3
10	9.71	1811.29	3
11	9.95	851.83	3
12	6.94	139.80	2
13	7	80.93	1
14	7.27	140.02	1
15	6.97	264.61	2
16	9.4	1388.91	3
17	6.6	79.99	1
18	6.64	66.83	1
19	8.61	220.96	1
20	7.6	42.03	1
21	9.85	2463.92	3
22	6.82	74.39	1
23	5.78	21.59	1
24	5.79	102.90	2
25	5	16.04	1
26	7.09	286.56	1
27	7.05	153.55	1
28	7.25	466.24	2
29	8.61	698.77	1
30	7.4	178.16	1
31	8.38	303.83	1
32	5.63	66.27	1
33	5.77	31.69	1
34	5.57	28.72	1
35	6.03	139.57	1
36	5.53	101.75	1
37	5.84	56.06	1

38	9.55	948.08	3
39	5.8	23.19	1
40	5.76	14.20	1
41	7.83	504.81	2
42	6.44	186.47	1
43	6.99	350.79	1
44	8.94	734.47	3
45	9.9	382.23	3
46	9.99	375.33	3
47	10.02	460.54	3
48	8.04	54.11	1
49	6.05	15.10	1
50	5.6	14.58	1
51	5.16	22.82	1
52	6.07	26.77	1
53	8.43	53.37	1
54	6.92	228.56	1
55	7.05	160.92	1
56	6.14	112.71	1
57	7.38	368.83	2
58	9.68	1941.77	3
59	7.25	212.38	1
60	6.78	154.90	2
61	10.09	836.79	3
62	7.03	236.04	1
63	6.91	171.18	2
64	6.99	193.81	2
65	5.92	58.56	1
66	9	301.94	1
67	5.84	25.51	1
68	5.7	32.79	1
69	6.96	109.94	1
70	6.96	148.06	1
71	6.74	123.08	1
72	6.42	79.17	1
73	6.74	90.53	2
74	6.37	65.76	1
75	6.87	53.13	1